Supporting Information for

Coordination Chemistry within a Protein Host: Regulation of the Secondary Coordination Sphere

Samuel I. Mann,[a] Tillmann Heinisch,[b] Thomas R. Ward,[b] and A. S. Borovik*[a]

[a]Department of Chemistry, University of California-Irvine, 1102 Natural Sciences II, Irvine, CA 92697
[b]Department of Chemistry, University of Basel, P.O. Box 3350, Mattenstrasse 24a, BPR 1096, CH-4002 Basel, Switzerland

Contents

General Methods. All commercially available reagents were obtained of the highest purity and used as received. Dimethylsulfoxide, *N*,*N*-dimethylformamide, and diethylether were degassed with argon and dried by vacuum filtration through activated alumina according to the procedure by Grubbs.[1] Triethylamine was distilled from KOH. Thin-layer chromatography (TLC) was performed on Whatman 250 μm layer 6 Å glass-backed silica gel plates. Eluted plates were visualized using UV light. Silica gel chromatography was performed with the indicated solvent system using Fisher reagent silica gel 60 (230-400 mesh). The ligands (biot-et-dpea and biot-pr-dpea) and Cu(II) complexes ([Cu^{II}(biot-et-dpea)(OH_2)Cl]Cl and [Cu^{II}(biot-pr-dpea)(OH_2)Cl]Cl) were prepared as previously published.[2] Sav mutants were expressed and purified as previously described.[3]

Physical Methods

Instrumentation. Electronic absorbance spectra were recorded with a 8453 Agilent UV-vis spectrophotometer. Circular dichroism (CD) spectra were collected on a Jasco J-810 spectropolarimeter equipped with a 163-900 nm laser. X-band (9.64 GHz) EPR spectra were recorded on a Bruker spectrometer equipped with Oxford liquid helium cryostats.

Electronic Absorption Studies. A typical azide titration experiment was performed using a 500 μL solution of 75 μM Sav prepared in 50 mM MES buffer, pH 6 in a low-volume 1 cm cuvette. 15 μL of a 10 mM solution of [Cu^{II}(biot-n-dpea(OH_2)Cl]Cl (n = et or pr) in DMF was added and allowed to equilibrate for 5 minutes. Azide was titrated 5 equivalents at a time (7.5 μL of a 1 M solution of NaN_3).

HABA Titrations. A 2.4 mL of a 8 μM solution of Sav in 200 mM phosphate buffer pH 7 was added to a 1 cm cuvette. 288 μL of a 10 mM (150 equivalents) HABA was added to ensure saturation of Sav. A 1 mM solution of [Cu^{II}(biot-n-dpea)(OH_2)Cl]Cl in DMF was added in 9.6 μL portions (0.5 equivalents) until 5 equivalents were added. The titration was monitored by UV-vis at λ_{max} = 506 nm (Fig. S12).

CD Studies. CD spectra were collected using a 500 μL solution of 75 μM Sav prepared in 50 mM MES buffer, pH 6. 15 μL of a 10 mM solution of [Cu^{II}(biot-n-dpea(OH_2)Cl]Cl (n = et or pr) in DMF was added and allowed to equilibrate for 5 minutes. 40 equivalents (6 μL) were added from a 1.0 M solution of NaN_3. Spectra were collected with the following parameters: data pitch: 0.5 nm, DIT: 4 s, bandwidth: 2 nm, speed: 50 nm/min, and 4 accumulations.

EPR Experiments. To 250 μL of a 250 μM solution of Sav in 50 mM MES buffer, pH 6.0 was added 25 μL of a 10 mM solution of [Cu^{II}(biot-n-dpea(OH_2)Cl]Cl (n = et or pr) in DMF. The solution was allowed to equilibrate for 5 minutes before addition of 40 equivalents of NaN_3 (10 μL of a 1 M solution). The solution was then transferred to an EPR tube and flash-frozen in liquid nitrogen.

Equilibrium Constant Determination.[4] To determine the effect of the H-bonding interaction on the binding affinity of azide to the anchored Cu complex, the binding equilibrium constants were determined for **1-N_3**, **1a-N_3**, **1b-N_3**, **2-N_3**, and **2a-N_3**. Azide binding studies were performed via addition of concentrated aqueous solutions of sodium azide to buffered solutions of Cu ArMs (see above). Despite being anchored within Sav, binding of the azide anion was rapid and

therefore no incubation was necessary before measurement. We did not try to achieve saturation of the ligand binding sites on the Cu center because formation of Cu-azide adducts with a greater than 1:1 stoichiometry was possible and difficult to differentiate from 1:1 binding modes. Additionally, the Sav host prohibits formation of azido-bridged dinuclear complexes. Following the methods described previously, the equilibrium constants were measured for each Cu ArM. Assuming 1:1 stoichiometry, the equilibrium constants can be determined using the following equilibrium expression:

$$K = \frac{[ML]}{[M][L]} = \frac{\Delta A}{(\Delta A_\infty - \Delta A)[L]} \quad (1)$$

where [M], [ML], and [L] are the concentrations of Cu ArM, Cu ArM azide adduct, and free azide, respectively. ΔA is the change in absorbance at the λ_{max} of the LMCT and ΔA_∞ is the absorbance change for complete formation of the 1:1 azide adduct. Equation 1 can be modified to give a double reciprocal plot:

$$\frac{1}{\Delta A} = \frac{1}{K\Delta A_\infty}\frac{1}{[L]} + \frac{1}{\Delta A_\infty} \quad (2)$$

Plotting $1/\Delta A$ versus $1/[L]$ should yield a straight line with a slope of $1/K\Delta A_\infty$ and x- and y-intercepts of $-K$ and $1/\Delta A_\infty$, respectively. Determining ΔA_∞ using this double reciprocal plot, the Hill equation can be used to confirm formation of 1:1 adducts:

$$\log\left[\frac{\Delta A}{(\Delta A_\infty - \Delta A)}\right] = n\log[L] + \log K \quad (3)$$

The slope of n = 1 for a plot of log $[\Delta A/(\Delta A_\infty - \Delta A)]$ versus log[L] indicates binding of a single azide ligand to the Cu center. Since the affinity for azide is low in these cases, it was assumed that the total azide concentration, $[L]_0$, is approximately equal to the free azide concentration ($[L]_0 \sim [L]$). The volume change in each solution was taken into account and the correlation coefficients for all lines fit in Excel were >0.99.

The UV-vis features of the N_3^- to Cu(II) LMCT, as well as the equilibrium constants (K) and *n* values for the Cu ArMs are summarized in Table S2. The Hill coefficients (*n*) were sufficiently close to 1 to assume formation of 1:1 Cu-N_3 adducts. Representative titrations and spectra can be found in Figures S3 and S9-S11. All titrations were performed in triplicate. The extinction coefficients in Table S2 are the extrapolated values calculated from ΔA_∞ from the double reciprocal plot. The optical activity of the LMCT band by CD was low, so numerical treatment of this titration data was unreliable. Instead, the spectra were measured with large excess of azide and those data are reported in Table S3.

Preparation of crystals of complex $[Cu^{II}(biot\text{-}pr\text{-}dpea)(OH_2)_2]^{2+} \subset$ WT Sav. Apo-Sav protein crystals were obtained at 20°C within two days by sitting-drop vapor diffusion technique mixing 1.5 μL crystallization buffer (2.0 M ammonium sulfate, 0.1 M sodium acetate, pH 4.0) and 3.5 μL protein solution (26 mg/mL lyophilized protein in water). The droplet was equilibrated against a reservoir solution of 100 μL crystallization buffer. Subsequently, single crystals of Sav were soaked for 1 day at 20 °C in a soaking buffer, which was prepared by mixing 1 μL of a 10

mM stock solution of complex [Cu^{II}(biot-pr-dpea(OH$_2$)Cl]Cl (in water with 100 mM CuCl$_2$), 9 μL crystallization buffer, and 0.5 μL of the original protein solution. After the soaking, crystals were transferred for 30 seconds into a cryo-protectant solution consisting of 30 % (v/v) glycerol in crystallization buffer. Next, crystals were shock-frozen in liquid nitrogen.

Preparation of crystals of complex [Cu^{II}(biot-n-dpea)(OH$_2$)N$_3$]$^{2+}$⊂WT Sav. Single crystals of [Cu^{II}(biot-n-dpea)(OH$_2$)$_2$]$^{2+}$⊂WT Sav (n = et or pr) were prepared as described above. The crystals were transferred to a solution of 1.0 mM NaN$_3$ in 30 % (v/v) glycerol for 5 minutes causing the crystals to turn from blue to green. The crystals were then shock-frozen in liquid nitrogen.

Data Processing. X-ray diffraction data were collected at the Stanford Synchrotron Radiation Lightsource (BL 14-1 and 9-2) at a wavelength of 1 Å and processed with software XDS[5] and scaled with AIMLESS (CCP4 Suite)[6]. The structure was solved by molecular replacement using program PHASER (CCP4 Suite)[6] and the structure 2QCB from the PDB as input model with ligand and water molecules removed. For structure refinement REFMAC5 (CCP4 Suite)[7] and PHENIX.REFINE[8] were used. Cu-complex manipulation was carried out with programs REEL and COOT using the Cu-complex coordinates of PDB structures 5K49 and 5K67 for ethyl and propyl linkers, respectively.[2] For water picking, electron density, and structure visualization, the software COOT[9] was used. Figures were drawn with PyMOL (the PyMOL Molecular Graphics System, Version 1.5.0.5, Schrödinger, LLC). Crystallographic details, processing and refinement statistics are given in Tables S4-S5.

Structural Results.

Crystal Color. All crystals of Sav soaked with complexes [Cu^{II}(biot-n-dpea(OH$_2$)Cl]Cl changed from colorless to pale blue (**1** and **2**) and from pale blue to green after soaking with azide (**1-N$_3$** and **2-N$_3$**).

Structural Refinement.

Overall Structures. Apo-crystals of proteins WT Sav soaked with Cu-complexes [Cu^{II}(biot-n-dpea(OH$_2$)Cl]Cl (n = et or pr) constituted space group I4$_1$22 with virtually identical unit cell parameters (Table S4). A single Sav monomer was obtained per asymmetric unit after molecular replacement. Protein residues 2-11 and 135-159 of the N- and C-terminus, respectively, were not resolved in the electron density, presumably due to disorder. Starting from the Sav monomer the biological homotetramer is generated by application of crystallographic C2-symmetry axes along the x-, y- and z-axes of the unit cell. The overall protein structures are virtually identical to structure biotin⊂WT Sav (PDB 1STP, see Table S4).

General Complex Modeling. For all structures of apo-protein crystals soaked with the corresponding Cu-complexes the following general observations were made: i) residual electron density in the F_o-F_c map was observed in the biotin binding pocket and in the biotin vestibule, which is flanked by protein residues of loop-3,4^A (the superscript number indicates Sav monomer within tetramer) loop-4,5^C, loop-5,6^A loop-7,8^A and loop-7,8^B, and iii) an anomalous dispersion density map indicated a significant peak in the biotin vestibule superimposed with the electron density peak (Figures S2 and S13). The residual electron density was fit with the corresponding Cu-complexes which projected Cu to the position of the strong anomalous density peak.

Structure Refinement of 1-N_3. The complex [Cu^{II}(biot-et-dpea)N_3]$^+$ was modeled with 100 % occupancy. The overall geometry of the Cu complex is similar to the previously published structure of **1**.[2] The coordinating pyridine nitrogen atoms of the dpea ligand were modeled as the axial ligands of a trigonal bipyramidal Cu-complex (Figure 3C-E, Figure S1, Table S1 and S4-S5). However, in contrast to (**1**), the aqua ligand pointing towards the biotin binding (O3) site is replaced by a stick-like density that was modeled as an azide ion. Only very weak electron density (< 3 σ) was observed in an F_o-F_c omit map in the third position of the trigonal plane suggesting that a water ligand in this position binds transiently. This aqua ligand is likely displaced due to photoreduction of the sample during data collection. We have shown previously that photoreduction does not cause significant changes to the metrical parameters for the remaining ligands.[10] One of the two pyridine rings (containing N3, N3 hereafter) of dpea is nestled within loop-7,8^A residues S112^A, T114^A, K121^A, L124^A and five water molecules (w66, w72, w136, 176, and w175^B) that form an H-bonding network. The second pyridine of dpea (containing N2, N2 hereafter) is in close proximity to loop-3,4^A and loop-7,8^B residues side chains N49^A and K121^B, as well as a glycerol molecule. The azido ligand is involved in H-bonds with N49^A and O1 (w66). The coordinated azido ligand is located near loop-5,6^C near side chain N49^A and O1 (w66). The Cu···Cu distance between two symmetry-related complexes is 11.3 Å (Figure S13). A free Cu ion was found near H87 from the crystal soaking condition and was modeled with 20% occupancy.

Structure refinement of complex 2-N_3: Except for the azide ligand the structure of complex [Cu^{II}(biot-pr-dpea(OH_2)N_3]$^+$⊂ Sav (**2-N_3**) is virtually identical to the structure of complex **2** (Figures 4, S2B-C, and S13B). The fourth ligand in the equatorial plane is occupied by an azide ligand. Due to the proximity of the symmetry-related Cu-complex pyridine the azide is slightly tilted out of the square plane (angle O_{aquo}–Cu-–N_{azide} = 148°). The Cu---N_{azide} distance is 1.9 Å. The distal azide nitrogen (N6) forms an H-bond with K121$_{N}\zeta$. A free Cu ion was found near H87 from the crystal soaking condition and was modeled with 50% occupancy.

Structure refinement of complex 2: In structure [Cu^{II}(biot-pr-dpea(OH_2)]$^{2+}$⊂Sav WT (**2**) the copper complex is fully occupied. The copper complex was modeled in a trigonal bipyramidal geometry (Figure 2, S2C and S13C). This is in stark contrast to the trigonal monopyramidal geometry of the corresponding complex [Cu^{II}(biot-pr-dpea)]$^+$ ⊂Sav S112C which was published earlier.[2] The nitrogens of the two pyridine rings are in axial position, the dpea tertiary amine and one aquo ligand is positioned in the trigonal equatorial plane. The aquo ligand points away from the neighboring Sav monomer. The Cu–O_{aquo} distance is 2.3 Å. Only very weak electron density (< 3 σ) was found in an F_o-F_c complex omit map in the remaining position within the trigonal plane that is facing towards the neighboring Sav monomer. This suggests transient binding of a water ligand in this position. This aqua ligand is likely displaced due to the photoreduction of the sample during data collection, as was discussed for **2-N_3**.[10] Note that two symmetry-related Cu-complex pyridine rings form a π-stacking interaction that presumably stabilizes the complex conformation (Fig. S13). Two neighboring Cu-complexes have a Cu---Cu distance of 7.2 Å. The conformation of the two symmetry-related complexes are further stabilized by hydrophobic interactions with residues L110^A, L110^B, K121^A, K121^B, L124^A and L124^B. An extended hydrogen bonding network including several water molecules is connecting the aqua ligand (O2) of the

Cu-complex with residues in loops 3,4, 5,6 and 7,8 (Figure 2A). A free Cu ion was found near H87 from the crystal soaking condition and was modeled with 50% occupancy.

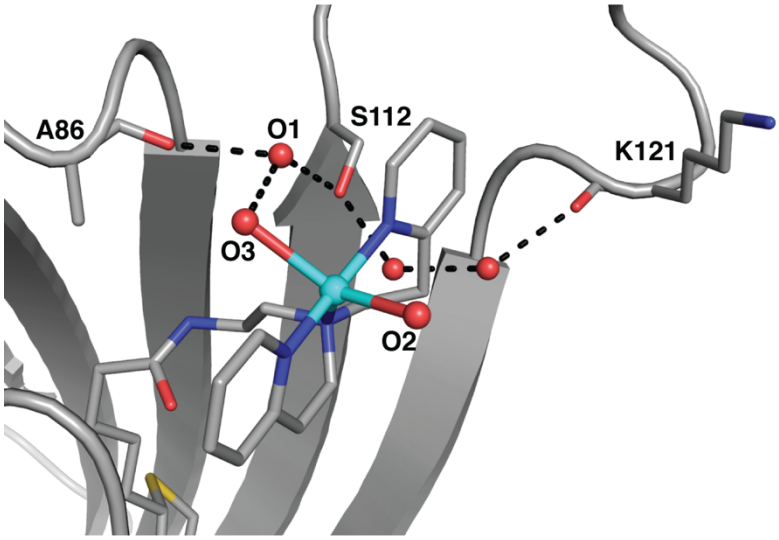

Figure S1. Molecular structure of **1** showing the extended H-bonding network that spans A86 to K121.

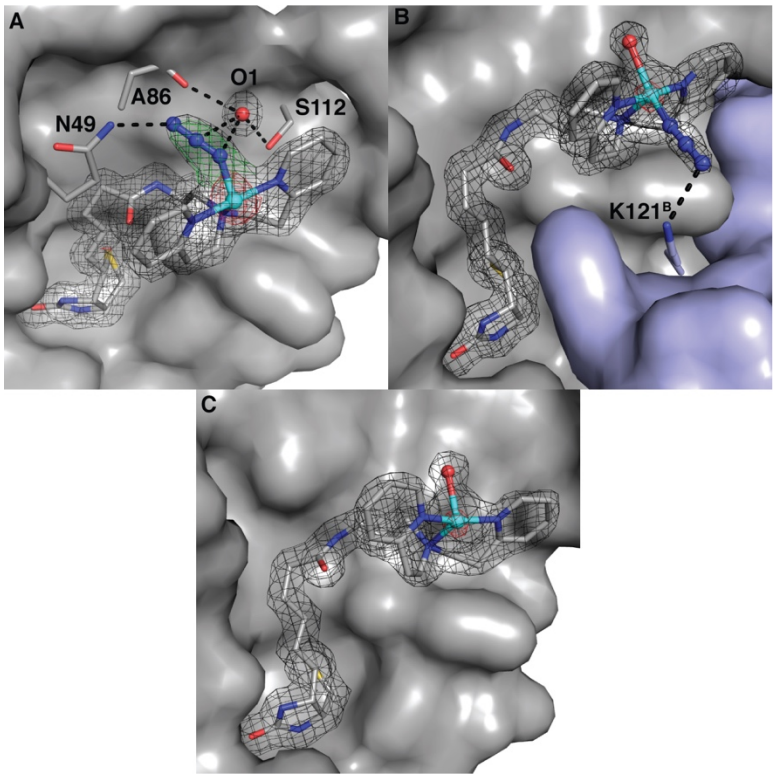

Figure S2. Close up views of the Cu complexes in crystal structures of **1**-N_3(**A**), **2**-N_3(**B**), and **2** (**C**). In (**B**) the adjacent subunit is in light blue. The position of the ligand molecules are indicated by the $2F_o$-F_c electron density (black mesh, contoured at 1σ) and anomalous difference density (red mesh, contoured at 7σ). In (**A**) the azido ligand is also shown with the F_o-F_c omit map (green mesh, contoured at 3σ). Copper ions are colored in cyan, oxygen atoms/water molecules are colored in red, and nitrogen atoms are colored in blue. Hydrogen bonding interactions are shown as dashed black lines.

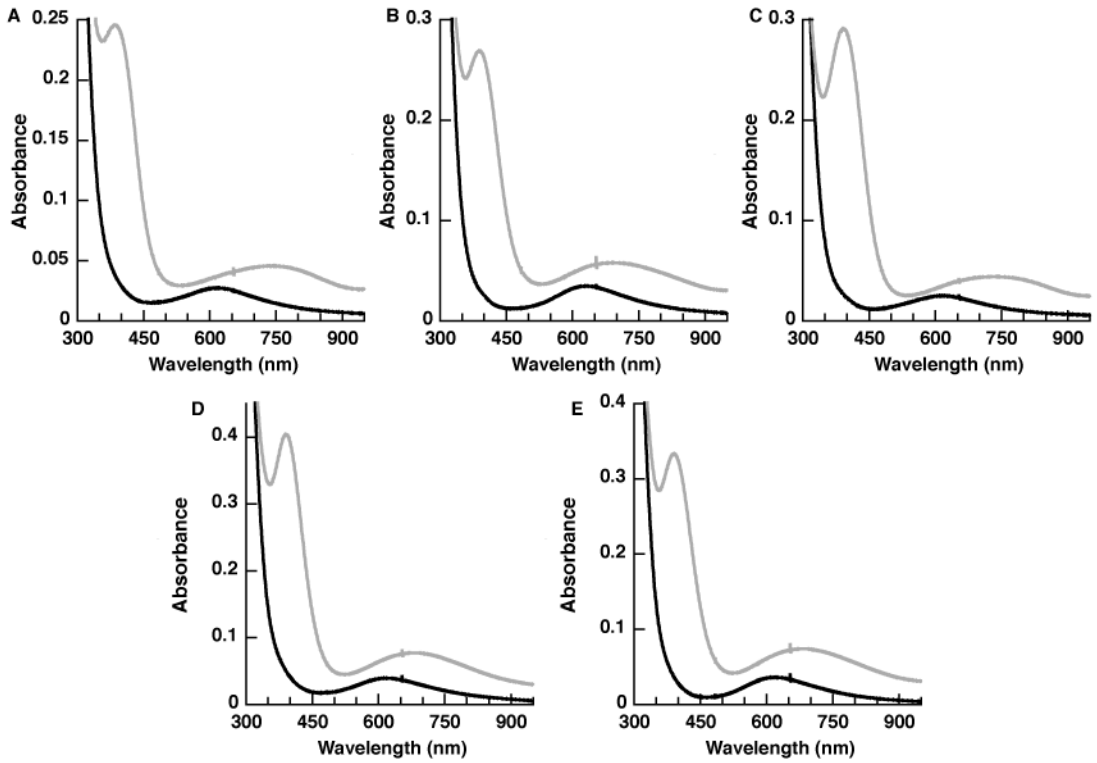

Figure S3. Absorption spectra before (black) and after addition of 40 equivalents azide (grey) for **1**/**1-N**$_3$ (A), **1a**/**1a-N**$_3$ (B), **1b**/**1b-N**$_3$ (C), **2**/**2-N**$_3$ (D), and **2a**/**2a-N**$_3$ (E).

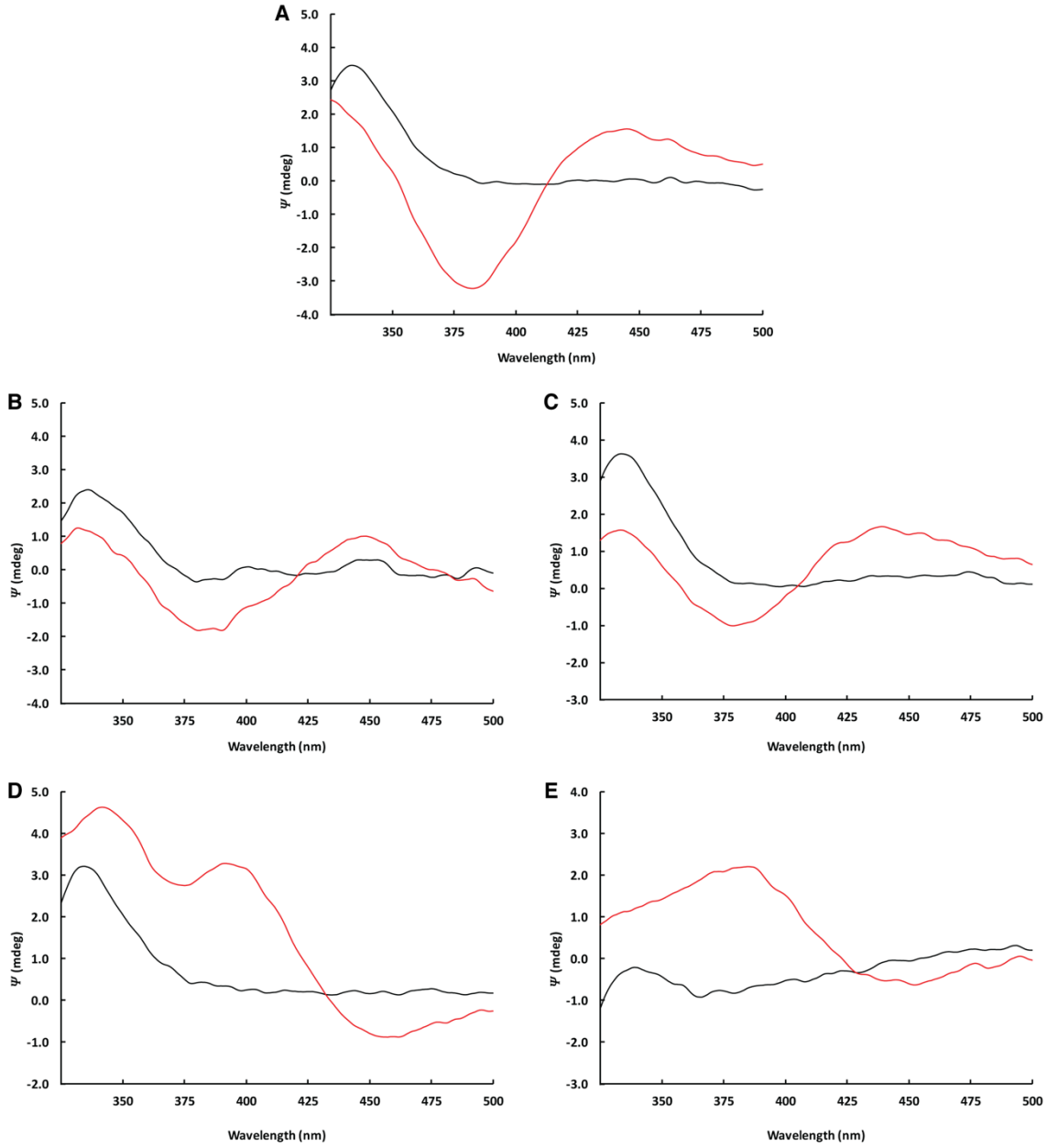

Figure S4. CD spectra for **1/1-N**$_3$ (A), **1a/1a-N**$_3$ (B), **1b/1b-N**$_3$ (C), **2/2-N**$_3$ (D), and **2a/2a-N**$_3$ (E), Initial spectrum (black) and final spectrum after 40 equivalents azide added (red).

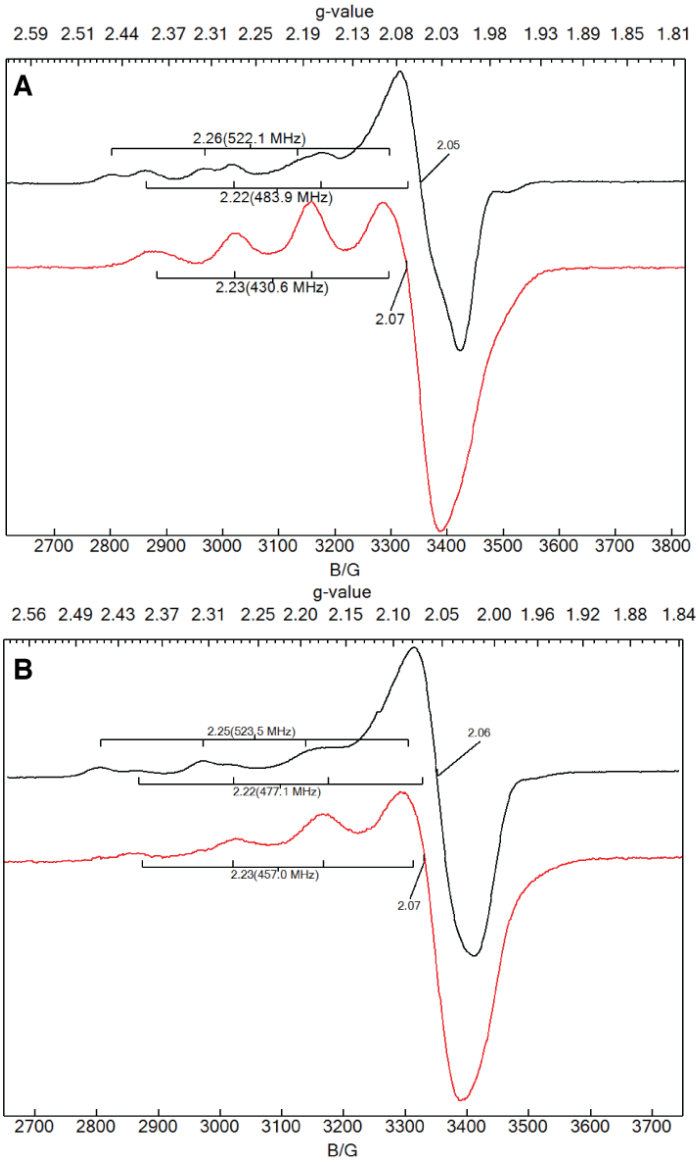

Figure S5. EPR spectra of (**A**) **1** (black) and **1**-N_3 (red) and (**B**) **2** (black) and **2**-N_3 (red).

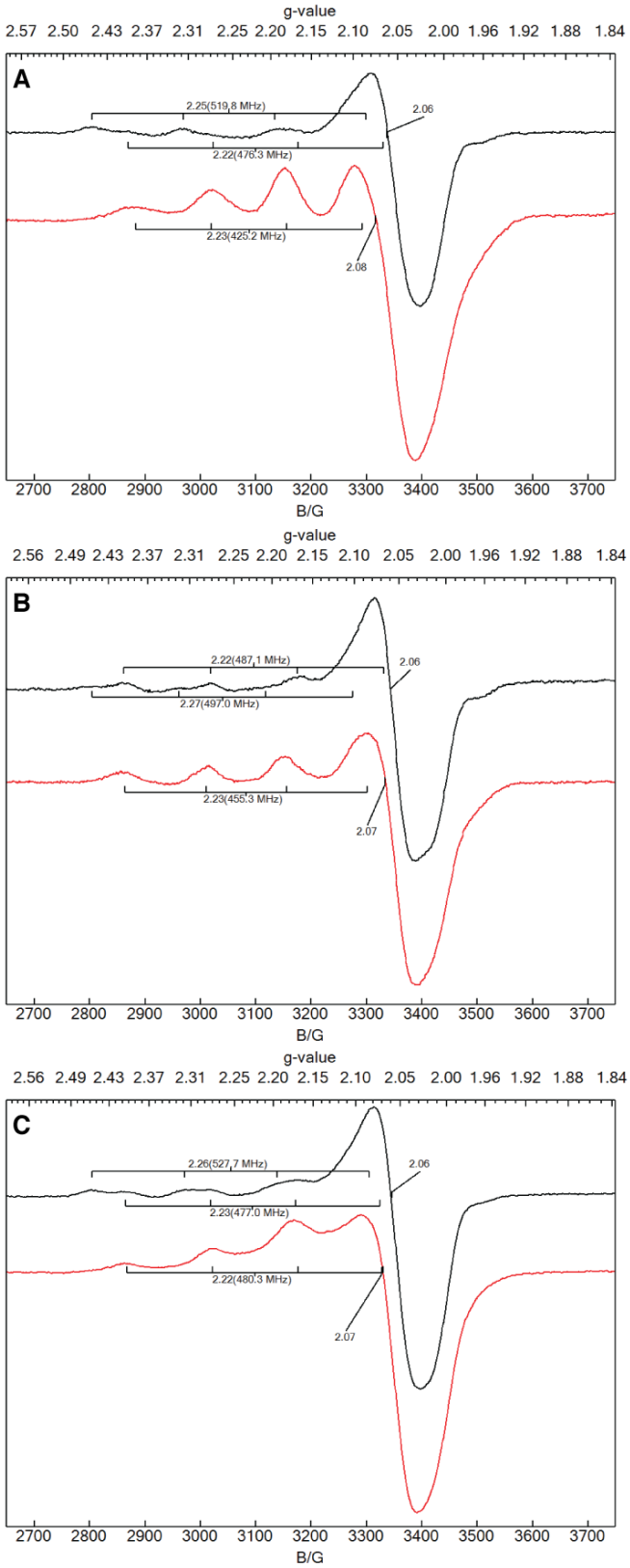

Figure S6. EPR spectra of (**A**) **1a** (black) and **1a**-N_3 (red), (**B**) **1b** (black) and **1b**-N_3 (red), and **2a** (black) and **2a**-N_3 (red).

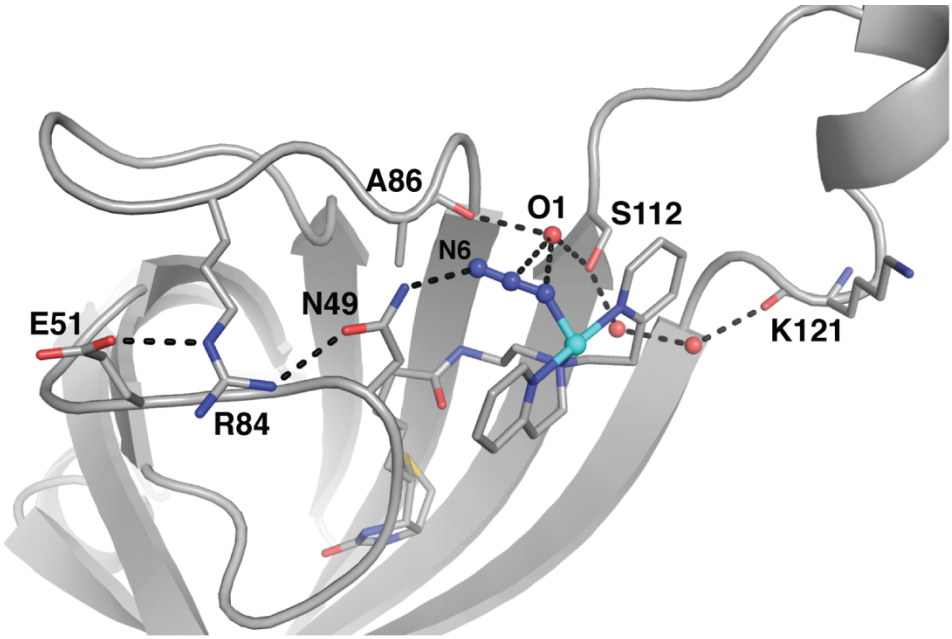

Figure S7. Structure of **1-N**, showing the extended H-bonding network that includes E51, R84, and N49.

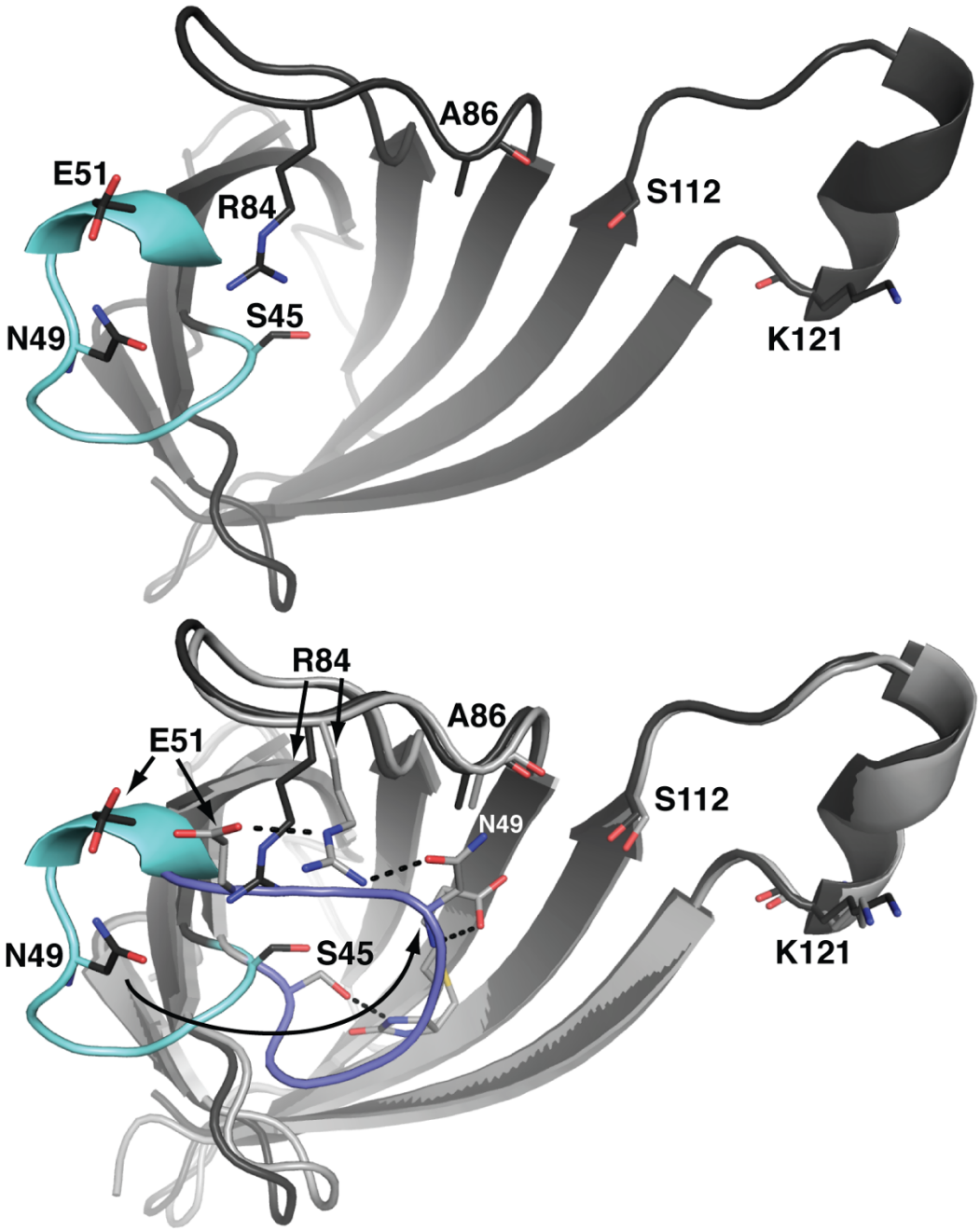

Figure S8. Structure of apo-Sav WT (top, PDB: 1SWC) with the flexible loop showin in teal and structure overlay (bottom) of apo-Sav WT (black) and biotin⊂Sav WT (grey, flexible loop is blue, PDB: 1SWE). Upon biotin binding, the flexible loop closes over biotin (teal to blue), S45 H-bonds to biotin, locking E51, R84, and N49 into an H-bonding network. H-bonds are showing as black dashed lines.

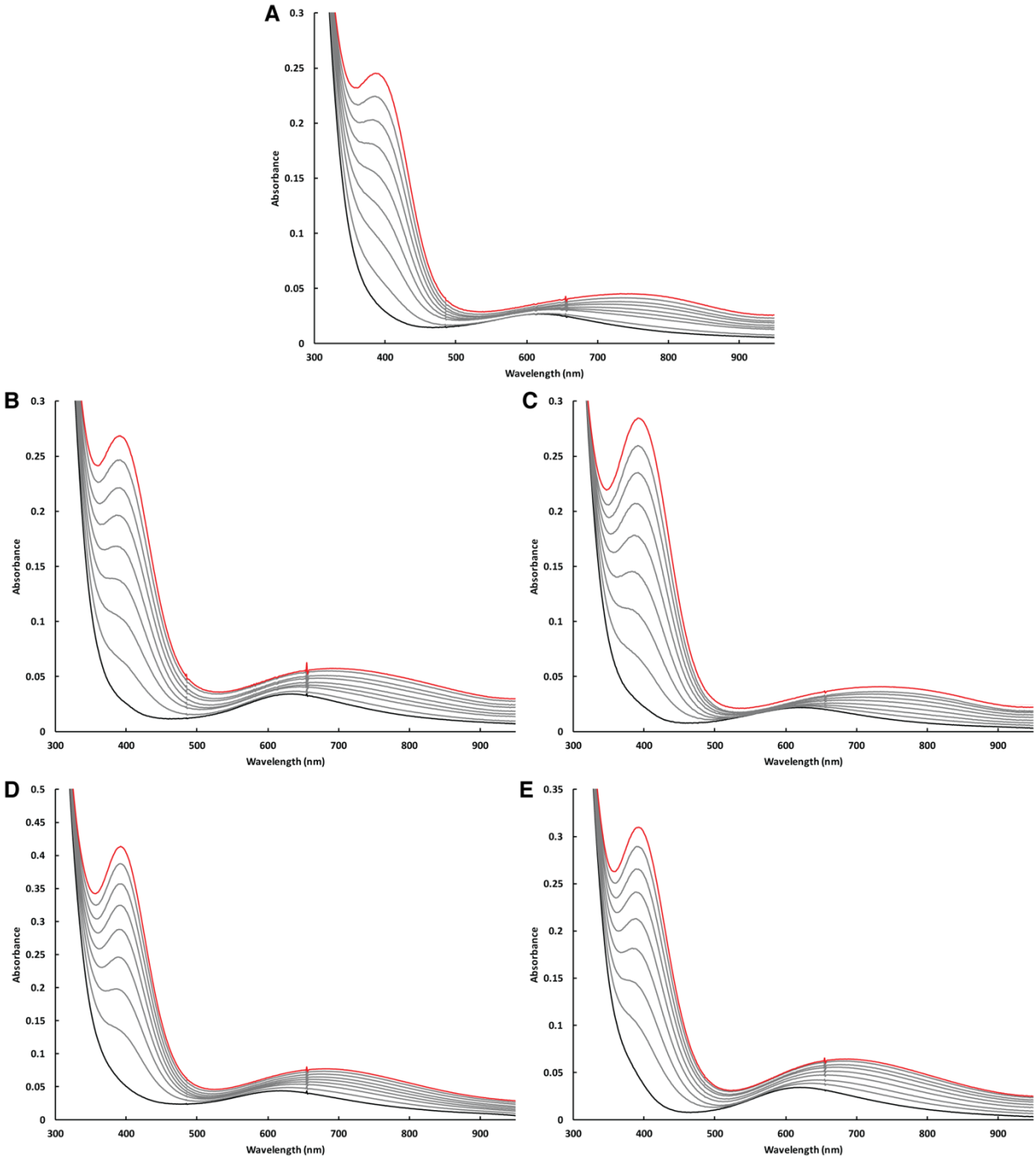

Figure S9. UV-vis titrations for **1**/**1-N**$_3$ (A), **1a**/**1a-N**$_3$ (B), **1b**/**1b-N**$_3$ (C), **2**/**2-N**$_3$ (D), and **2a**/**2a-N**$_3$ (E), Initial spectrum (black), titrations of 5 equivalents at a time (grey), and final spectrum after 40 equivalents added (red).

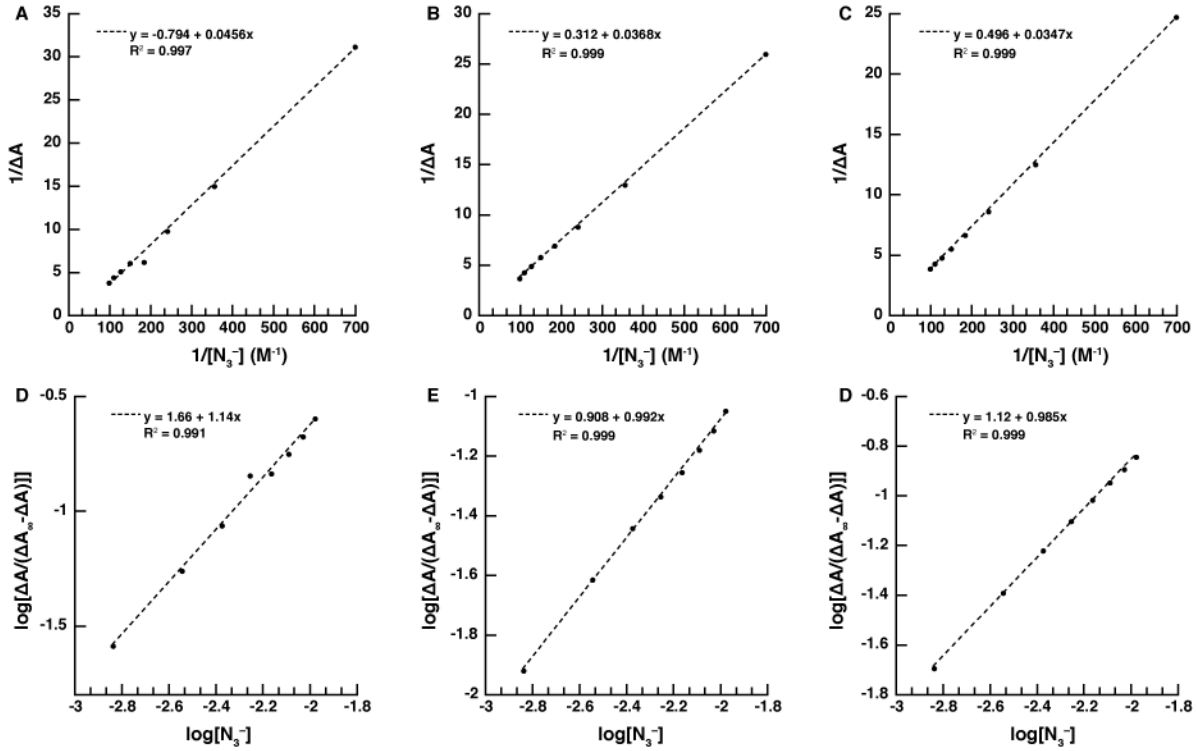

Figure S10. Double-reciprocal plots for **1-N**$_3$ (A), **1a-N**$_3$ (B), and **1b-N**$_3$ (C). Hill equation plots for **1-N**$_3$ (D), **1a-N**$_3$ (E), and **1b-N**$_3$ (F).

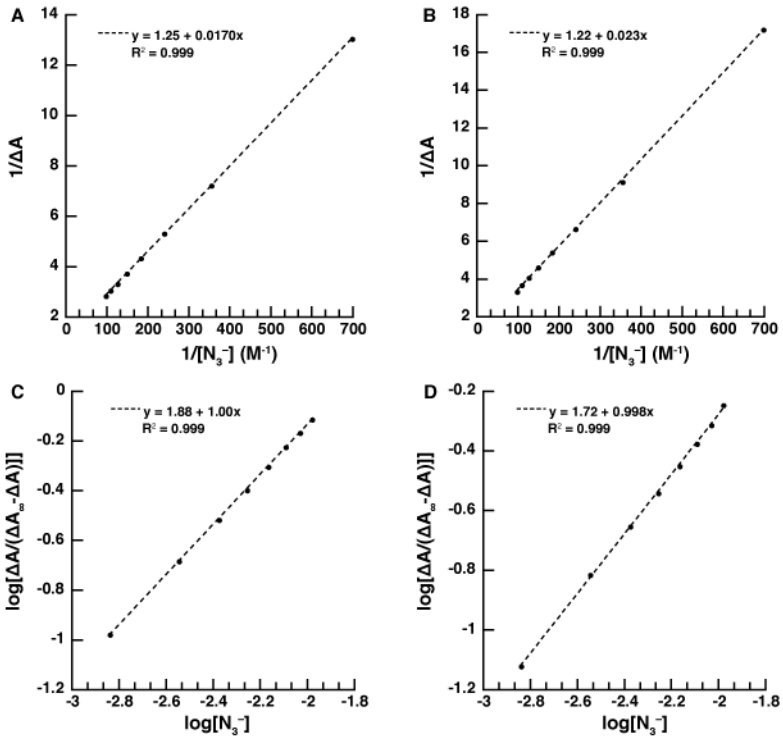

Figure S11. Double-reciprocal plots for **2-N**$_3$ (A) and **2a-N**$_3$ (B). Hill equation plots for **2-N**$_3$ (D) and **2a-N**$_3$ (E).

Table S1. Selected Bond Lengths (Å) and Angles (°) for **1**, **1**-N_3, **2**, and **2**-N_3.

Metrical Parameters	1	1-N_3	2	2-N_3
Cu–N1	2.08(3)	2.10(3)	2.17(2)	2.14(3)
Cu–N2	2.02(3)	1.99(3)	2.07(2)	2.13(3)
Cu–N3	2.09(3)	2.11(3)	2.10(2)	2.04(3)
Cu–N4	–	1.88(3)	–	1.87(3)
Cu-O2	2.46(3)	–	2.32(2)	2.29(3)
Cu-O3	2.52(3)	–[a]	–[a]	–
τ_5	0.72	–[a]	–[a]	0.52
N1–Cu–N2	102(3)	97(3)	94(3)	93(3)
N1–Cu–N3	88(3)	84(3)	101(3)	88(3)
N1–Cu–N4	–	106(3)	–	112(3)
N2–Cu–N3	170(3)	178(3)	165(3)	178(3)
N2–Cu–N4	–	95(3)	–	68(3)
N3–Cu–N4	–	87(3)	–	110(3)
N1–Cu–O2	127(3)	–	100(3)	96(3)
N2–Cu–O2	84(3)	–	91(3)	95(3)
N3–Cu–O2	88(3)	–	87(3)	86(3)
N4–Cu–O2	–	–[a]	–[a]	147(3)
N1–Cu–O3	104(3)	–[a]	–[a]	–
N2–Cu–O3	86(3)	–[a]	–[a]	–
N3–Cu–O3	94(3)	–[a]	–[a]	–

[a] aquo ligand in trigonal plane not visible in electron density of F_o-F_c omit map

Table S2. UV-vis Spectroscopic Properties, Equilibrium Constants, and Hill Coefficients for ArMs.

ArM	Abs λ_{max}, nm (ε, M^{-1} cm^{-1})[a]	K (M^{-1})[c]	*n*
1	625 (90)	–	–
1-N$_3$	390 (6000) 750 (390)	23 ± 4	1.2
1a	634 (120)	–	–
1a-N$_3$	390 ([b]) 702 ([b])	6 ± 2	0.99
1b	616 (80)	–	–
1b-N$_3$	389 ([b]) 750 ([b])	12 ± 2	0.99
2	625 (100)	–	–
2-N$_3$	393 (3200) 698 (290)	68 ± 5	0.98
2a	620(120)	–	–
2a-N$_3$	390 (3300) 690 (290)	56 ± 3	0.99
[Cu^{II}(biot-et-dpea(OH$_2$)N$_3$]$^+$	386 (2050) 694 (270)	193 ± 3	1.0
[Cu^{II}(biot-pr-dpea(OH$_2$)N$_3$]$^+$	386 (2000) 697 (300)	190 ± 4	1.0

[a]extinction coefficients were calculated from extrapolated maximum intensities at infinite azide concentrations; [b]extinction coefficients were unable to be calculated due to poor azide binding; [c] measured at 294 K.

Table S3. CD and EPR parameters for Cu ArMs.

Host	WT				N49A		S112A		K121A	
n	et (1)	pr (2)	et (1-N_3)	pr (2-N_3)	et (1a)	et (1a-N_3)	et (1b)	et (1b-N_3)	pr (2a)	pr (2a-N_3)
CD λ_{max},nm	333	335	324 382 445	342 392 457	336	332 390 448	334	334 379 439	339	385 452
g	2.05 2.22 2.26	2.06 2.22 2.25	2.07 2.23	2.08 2.23	2.06 2.22 2.25	2.08 2.23	2.06 2.22 2.27	2.07 2.23	2.06 2.23 2.26	2.07 2.22
A, MHz	522 484	477 524	430	457	476 520	425	487 497	455	477 528	480

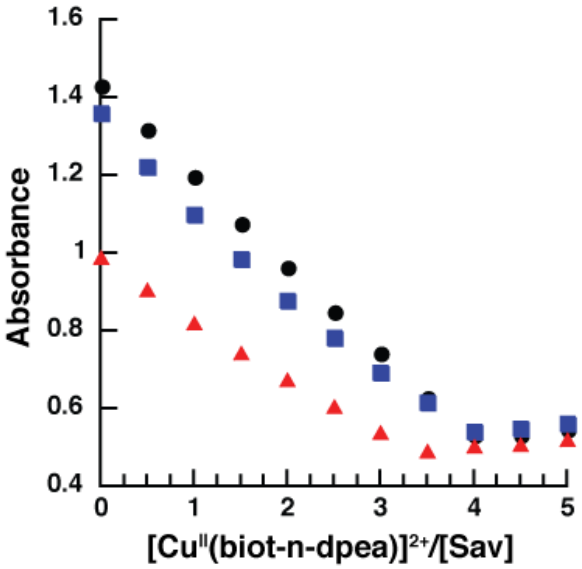

Figure S12. HABA titrations for **1a** (black circles), **1b** (blue squares), and **2a** (red triangles).

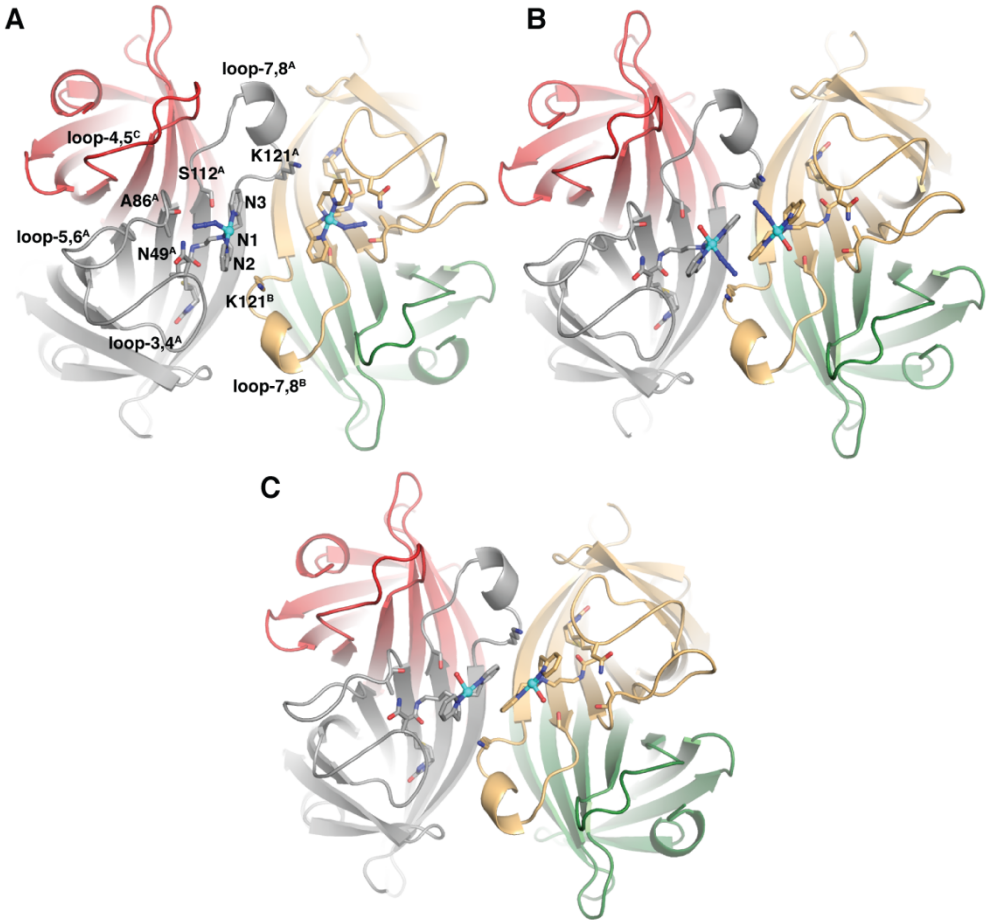

Figure S13. Views of the structures of **1**-N_3(**A**), **2**-N_3(**B**), and **2** (**C**). The Sav tetramers are represented as a cartoon and the cofactors are represented as ball and stick. Subunit A is in grey, subunit B is in tan, subunit C is in red, and subunit D is in green.

Table S4. X-ray crystallography data processing and refinement statistics.

Sav Mutant	WT	WT	WT
Cu complex	[Cu^{II}(biot-pr-dpea)(OH_2)]$^{2+}$ (**1b**)	[Cu^{II}(biot-pr-dpea)(OH_2)N_3]$^{+}$ (**1b-N_3**)	[Cu^{II}(biot-et-dpea)(OH_2)N_3]$^{+}$ (**1a-N_3**)
PDB code	5VL8	5VL5	5VKX
Cu complex PDB 3-letter code	S32	S31	S18
Data Processing			
Unit Cell	a, b, c = 57.6 Å, 57.6 Å, 183.6 Å; α, β, γ = 90°	a, b, c = 57.7 Å, 57.7 Å, 183.6 Å; α, β, γ = 90°	a, b, c = 57.9 Å, 57.9 Å, 184.4 Å; α, β, γ = 90°
Space group	$I4_122$	$I4_122$	$I4_122$
Resolution (Å)	54.9 – 1.70	55.1 – 1.46	37.4 – 1.37
Highest resolution shell (Å)	1.73 - 1.70	1.49 – 1.46	1.40 – 1.37
R_{merge} (%)	12.7 (129.3)	18.8 (148.3)	4.9 (96.2)
No. of unique reflections	17570 (904)	27425 (1349)	33187 (1457)
Multiplicity	8.7 (6.1)	8.1 (7.6)	11.1 (7.7)
I/sig(I)	9.3 (1.0)	3.9 (0.5)	22.2 (1.4)
Completeness	100 (100)	100 (100)	99.5 (90.8)
CC(1/2)	0.997 (0.27)	0.99 (0.62)	1.00 (0.74)
Structure Refinement			
R_{work}	0.18	0.23	0.16
R_{free}	0.21	0.26	0.19
Rmsd bond length (Å)	0.021	0.025	0.031
Rmsd bond angle (°)	3.431	3.242	2.874
Rmsd compared to biotin-SAV WT (PDB 1STP) (Å)	0.71	0.70	0.73
<u>No. ligands</u> Cu complex Water Glycerol Cu(B)	 1 146 1 1	 1 152 - 1	 1 178 1 1

Table S5. Summary of structural details.

PDB code	5VL8	5VL5	5VKX
Complex	**1b**	**1b-N_3**	**1a-N_3**
Electron density at Cu in FoFc omit map (σ)	21	20	28
Anomalous dispersion density at Cu (σ)	15	11	26
Geometry of Cu complex	Trigonal bipyramidal*	Distorted square pyramidal	Trigonal bipyramidal*
Coordination number of Cu complex	5*	5	5*
Occupancy of Cu complex (%)	100	100	100
B-factor (Å^2)			
Overall protein	25.5	23.0	20.6
Loop 7,8	25.3	22.7	20.0
Loop 3,4	25.0	23.6	20.3
Cu complex	29.8	28.4	26.5
DPEA	29.5	27.7	24.8
Cu	36.0	34.4	32.3
N_3^-	–	32.6	44.6
Distance Cu-Cu (Å)	7.2	7.3	11.3

*Aquo ligand in equatorial plane was only weakly visible (< 3 σ) in electron density of F_o-F_c omit map.

References.

1 A. B. Pangborn, M. A. Giardello, R. H. Grubbs, R. K. Rosen and F. J. Timmers, *Organometallics*, 1996, **15**, 1518–1520.

2 S. I. Mann, T. Heinisch, A. C. Weitz, M. P. Hendrich, T. R. Ward and A. S. Borovik, *J. Am. Chem. Soc.*, 2016, **138**, 9073–9076.

3 H. Mallin, M. Hestericová, R. Reuter and T. R. Ward, *Nat. Protoc.*, 2016, **11**, 835–852.

4 L. Casella, M. Gullotti, G. Pallanza and M. Buga, *Inorg. Chem.*, 1991, **30**, 221–227.

5 W. Kabsch, *Acta Crystallogr. D. Biol. Crystallogr.*, 2010, **66**, 125–132.

6 P. R. Evans, *Acta Crystallogr. Sect. D Biol. Crystallogr.*, 2011, **67**, 282–292.

7 G. N. Murshudov, A. A. Vagin and E. J. Dodson, *Acta Crystallogr. D. Biol. Crystallogr.*, 1997, **53**, 240–255.

8 P. D. Adams, P. V Afonine, G. Bunkóczi, V. B. Chen, I. W. Davis, N. Echols, J. J. Headd, L.-W. Hung, G. J. Kapral, R. W. Grosse-Kunstleve, A. J. McCoy, N. W. Moriarty, R. Oeffner, R. J. Read, D. C. Richardson, J. S. Richardson, T. C. Terwilliger and P. H. Zwart, *Acta Crystallogr. D. Biol. Crystallogr.*, 2010, **66**, 213–221.

9 P. Emsley and K. Cowtan, *Acta Crystallogr. D. Biol. Crystallogr.*, 2004, **60**, 2126–2132.

10 S. I. Mann, T. Heinisch, T. R. Ward and A. S. Borovik, *J. Am. Chem. Soc.*, 2017, jacs.7b10452.